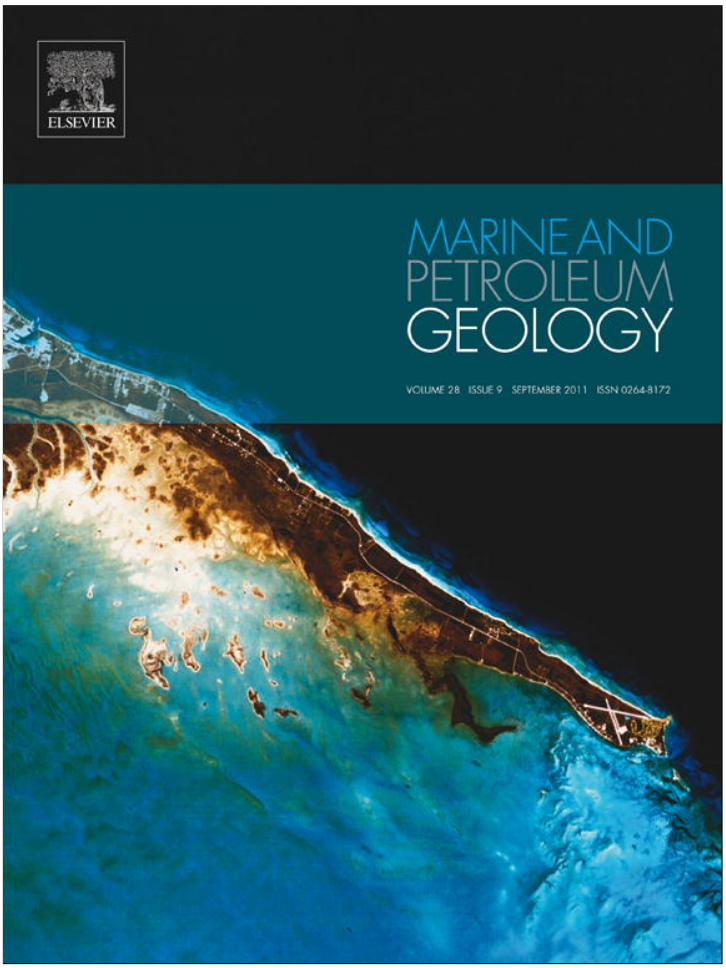

Marine and Petroleum Geology 28 (2011) 1611–1624

Contents lists available at ScienceDirect

Marine and Petroleum Geology

journal homepage: www.elsevier.com/locate/marpetgeo

Geochemical characteristics and hydrocarbon generation modeling of the Jurassic source rocks in the Shoushan Basin, north Western Desert, Egypt

Mohamed Ragab Shalaby [a], Mohammed Hail Hakimi [a,b,*], Wan Hasiah Abdullah [a]

[a] Geology Department, University of Malaya, 50603 Kuala Lumpur, Malaysia
[b] Geology Department, Faculty of Applied Science, Taiz University, 6803 Taiz, Yemen

ARTICLE INFO

Article history:
Received 26 March 2011
Received in revised form
21 June 2011
Accepted 9 July 2011
Available online 21 July 2011

Keywords:
Organic geochemistry
Jurassic
Hydrocarbon generation
Shoushan Basin
Egypt

ABSTRACT

The Shoushan Basin is an important hydrocarbon province in the Western Desert, Egypt, but the origin of the hydrocarbons is not fully understood. In this study, organic matter content, type and maturity of the Jurassic source rocks exposed in the Shoushan Basin have been evaluated and integrated with the results of basin modeling to improve our understanding of burial history and timing of hydrocarbon generation. The Jurassic source rock succession comprises the Ras Qattara and Khatatba Formations, which are composed mainly of shales and sandstones with coal seams. The TOC contents are high and reached a maximum up to 50%. The TOC values of the Ras Qattara Formation range from 2 to 54 wt.%, while Khatatba Formation has TOC values in the range 1–47 wt.%. The Ras Qattara and Khatatba Formations have HI values ranging from 90 to 261 mgHC/gTOC, suggesting Types II-III and III kerogen. Vitrinite reflectance values range between 0.79 and 1.12 VRr %. Rock–Eval T_{max} values in the range 438–458 °C indicate a thermal maturity level sufficient for hydrocarbon generation. Thermal and burial history models indicate that the Jurassic source rocks entered the mature to late mature stage for hydrocarbon generation in the Late Cretaceous to Tertiary. Hydrocarbon generation began in the Late Cretaceous and maximum rates of oil with significant gas have been generated during the early Tertiary (Paleogene). The peak gas generation occurred during the late Tertiary (Neogene).

1. Introduction

The Western Desert of Egypt (Fig. 1) still has a significant hydrocarbon potential as recent oil and gas discoveries have suggested (Dolson et al., 2001) with as much as 90% of oil reserves and 80% of gas in the Western Desert's Basins yet to be discovered (Zein El-Din et al., 2001). Recent hydrocarbon discoveries that have been made in the Abu Gharadig Basin and the Shoushan Basin to the NW are thought to have significant exploration potential (EGPC, personal communication, 1992 "personal communication"). The area that forms the scope of this study lies in the Shushan Basin (Fig. 1). The study area occupies the Eastern part of the Shoushan Basin, which lies between latitudes 30° 30′ – 31° 00′ N and longitudes 26° 30′ – 27° 00′ E (Fig. 1) and has attracted the interest of numerous researchers and oil companies for exploration of hydrocarbons. The presence of possible source rocks in the Shoushan Basin occurs in the Jurassic, Cretaceous, and Paleozoic rock units (El Ayouty, 1990; Ghanem et al., 1999; Khaled, 1999; Sharaf, 2003; El-Nadi et al., 2003; Alsharhan and Abd El-Gawad, 2008). The Jurassic organic-rich sediments of the Ras Qattara and Khatatba Formations are considered to be the most prolific oil and gas prone source rocks in the basin. However, few studies have investigated the geochemical characteristics of the source rocks or their thermal and burial histories, and the timing of hydrocarbon generation is therefore poorly understood. The objective of this study was to evaluate the organic matter content, type and thermal maturity of the source rocks and to incorporate the results into basin modeling in order to know and determine the timing of hydrocarbon generation. Maturity information was used for calibration of numerical models. Burial history, thermal maturity and timing of hydrocarbon generation and expulsion were modeled for the Ras Qattara and Khatatba Formations source rocks at two exploration wells.

2. Geological setting

The northern Western Desert of Egypt is characterized by a Paleozoic section overlying crystalline basement, and a northward-thickening prism of Mesozoic and Tertiary strata. The

* Corresponding author. Geology Department, University of Malaya, 50603 Kuala Lumpur, Malaysia
E-mail address: ibnalhakimi@yahoo.com (M. H. Hakimi).

0264-8172/$ – see front matter © 2011 Elsevier Ltd. All rights reserved.
doi:10.1016/j.marpetgeo.2011.07.003

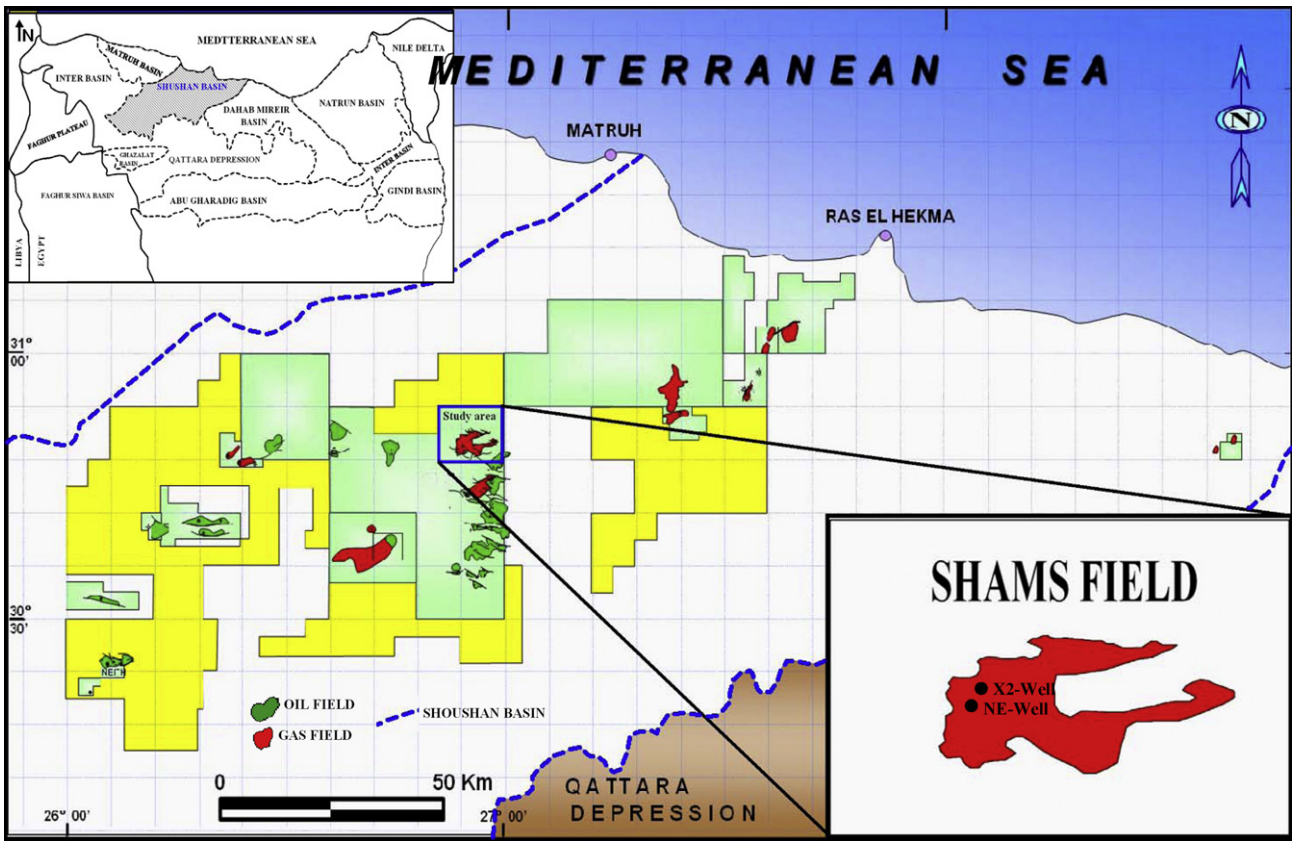

Figure 1. Location of Shams Field in the Shushan Basin, Western Desert, Egypt (modified after EGPC, 1992 "personal communication").

structural grain of the basement is dominated by two orthogonal trends induced by successive diastrophic phases. During Paleozoic time, at least two phases of Major deformation produced an N to NW trending system of block faulting and gentle folding with marked unconformities within the Paleozoic section. The Mesozoic–Tertiary sedimentary wedge is interrupted by an east–west trending structural high, which separates the Abu Gharadig basin from a series of coastal basins (Fig. 1). This pattern of basins and highs is masked under gently dipping, outcropping Miocene deposits (El Ayouty, 1990; Kerdany and Cherif, 1990). The coastal basins started as rifts during the early Mesozoic in association with the opening of the Tethys. Structures result primarily from vertical movement of basement blocks, and consist of draped over and/or faulted anticlinal features (Fig. 2). Compressional anticlines are subordinate and probably derive from drag folding, related to lateral movement along basement faults. The structures in the north Western Desert, focusing on the Shoushan Basin, consists mainly of parallel, elongated, titled fault blocks, that is, horst and half-graben structures, with associated erosion of the upthrown blocks (Fig. 2). The Shoushan Basin, which is the largest of the coastal basins, is a half-graben system with a maximum thickness of 7.5 km of Jurassic, Cretaceous and Paleogene sediments (El Shazly 1977; Hantar, 1990).

The northern Western Desert consists of a number of sedimentary basins that received a thick succession of Mesozoic sediments. Lithostratigraphic units in these basins have been studied by many authors who have discussed the stratigraphy, facies and tectonic framework of the region (e.g., Abdine and Deibis, personal communication, 1972 "personal communication"; Mesherf et al., 1980; Barakat et al., 1987). The stratigraphic section in the northern Western Desert (including Shoushan Basin) ranges in age from Paleozoic to Tertiary and is summarized in Fig. 3. The stratigraphy can be divided into four unconformity-bound cycles as proposed by Sultan and Abdulhalim (personal communication, 1988). The earliest cycle consists of Lower Jurassic non-marine siliciclastics (Ras Qattara Formation) which rest unconformably on the Paleozoic Nubian sandstone and is overlain by the Mid-Jurassic Khatatba Formation. The Khatatba Formation is composed mainly of shales and sandstones with coal seams. These sediments were deposited in a deltaic to shallow marine environments. In the Upper Jurassic, shallow-marine carbonates of the Masajid Formation were deposited and represent the maximum Jurassic transgression. The Masajid Formation was either eroded from, or was not deposited on parts of the north Qattara Ridge and Umbarka Platform, although continuous marine sedimentation occurred in the Matruh (sub)-basin. A major unconformity separates the Masajid Formation from the overlying Alam El Bueib Formation at the base of the second cycle, whose basal interval is composed of Early Cretaceous shallow-marine sandstones and carbonates (Units 6 and 5). These are followed by marine shale (Unit 4) and a succession of massive fluvial sandstones (Units 3; Neocomian). Individual sand bodies are separated by marine shale. The sands are overlain by the alternating sands, shales and shelf carbonates of Units 2 and 1, culminating in the Alamein dolomite associated with the Aptian transgression (Fig. 2). The Dahab Shale marks the end of this cycle. The continental and shoreline sandstones of the Kharita Formation are overlain by the shallow-marine and nearshore deposits of the Bahariya Formation (Lower Cenomanian). A marked deepening of depositional conditions is indicated by the deposition of the Abu Roash (G) (Upper Cenomanian). Widespread transgression occurred during the Senonian with deposition of the Abu Roash (F) to (A) (predominantly carbonates). The unconformably overlying Khoman Chalk Formation was deposited only in the northern Western Desert. The cycle is

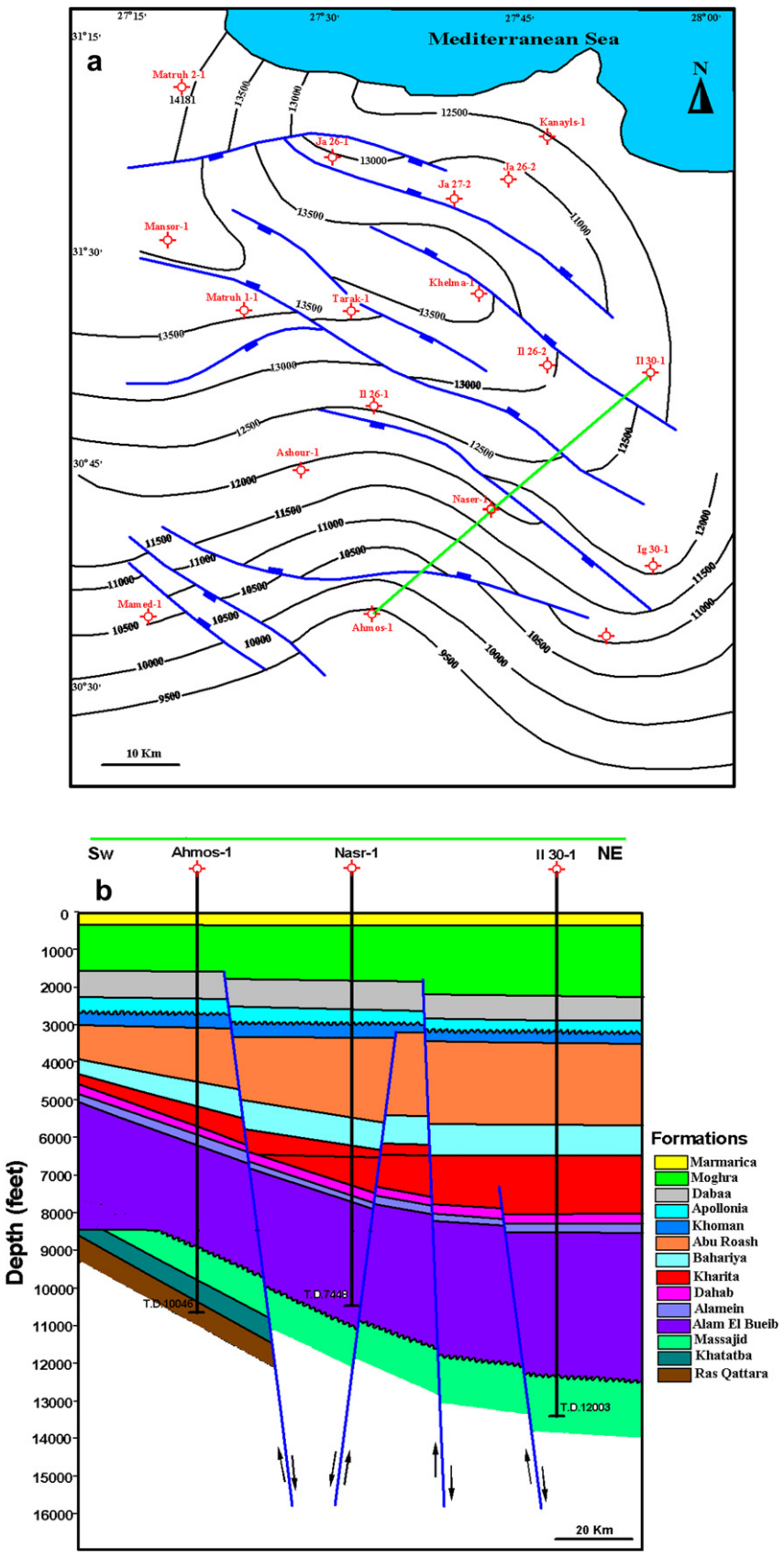

Figure 2. Structural setting of the Shoushan Basin, Western Desert; (a) structure contours at top Khatatba Formation (modified after Robertson, 1982"personal communication"); (b) Subsurface cross section shows faults pattern in the Shoushan Basin, faults identified from seismic (modified after Alsharhan and Abd El-Gawad, 2008).

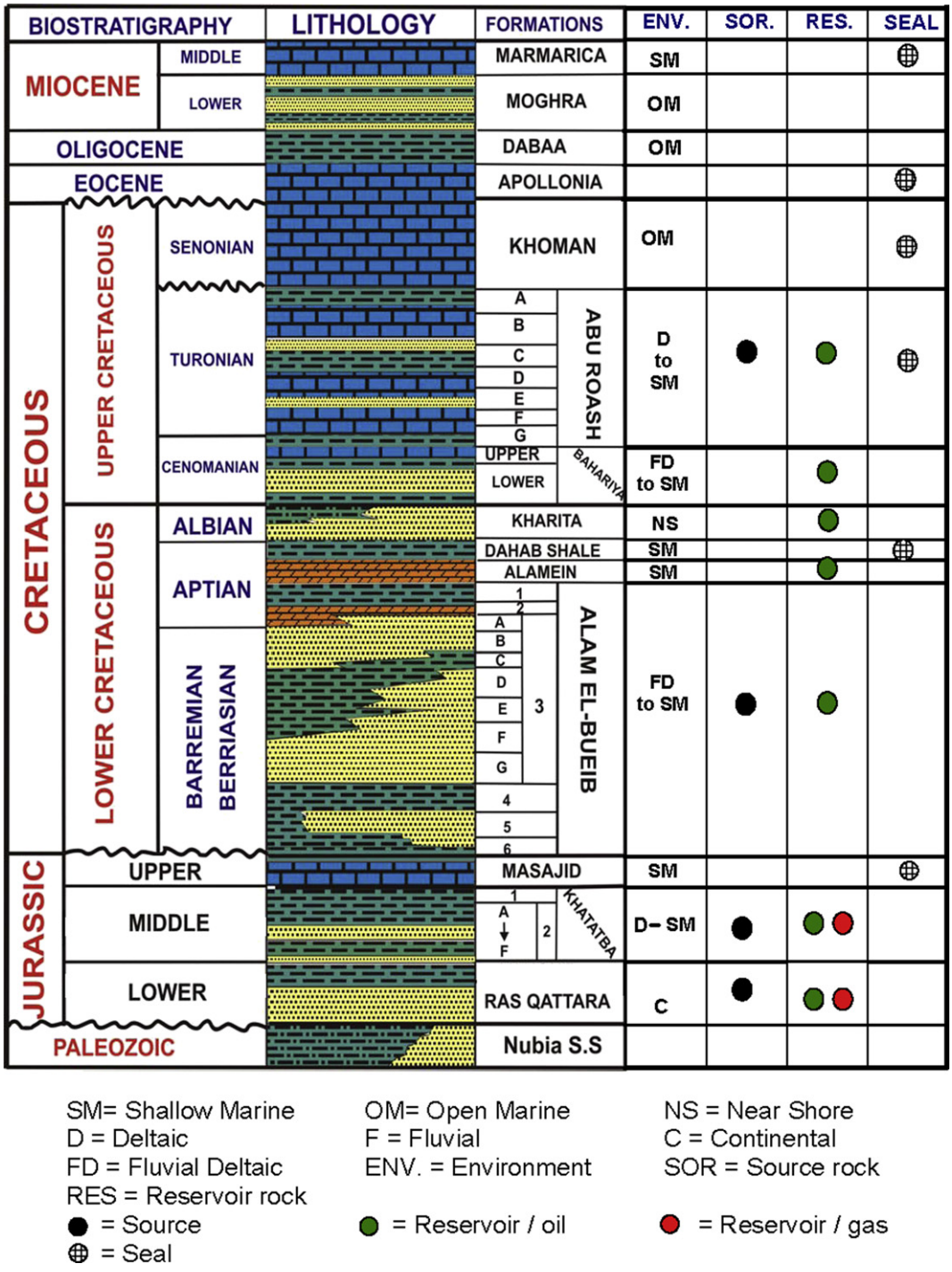

Figure 3. Regional stratigraphic nomenclature, Western Desert including Shushan Basin, Egypt (modified after Schlumberger, 1984, 1995"personal communication").

terminated by an unconformity, above which the Eocene Apollonia Formation was deposited. The Dabaa and Moghra Formations (marine clastics) above the Apollonia Formation are capped by the Marmarica Limestone (Zein El-Din et al., 2001).

3. Samples and methods

A total of 69 samples from Jurassic rocks (39 samples from Khatatba Formation and 30 samples from Ras Qattara Formation) were collected from two wells in the Shams field, Shoushan Basin (Fig. 1).

3.1. Analytical procedures

Geochemical analyses were performed on the Jurassic Ras Qattara and Khatatba Formations samples from the two wells (Tables 2 and 3). Pyrolysis analyses were conducted using a Rock-Eval II unit with a total organic carbon module. Parameters measured include TOC, S_1, S_2, S_3 and temperature of maximum pyrolysis yield (T_{max}). Hydrogen Index (HI) and Oxygen Index (OI) were calculated as described by Espitalié et al. (1977) and Peters and Cassa (1994). Rock-Eval S_2 yields are a useful measurement of the generative potential of source rocks (Peters, 1986; Bordenave, 1993). S_2 yields

Table 1
Input data used for modeling of hydrocarbons generation and expulsion in the studied wells.

Formation	Deposition age (Ma)		Lithology	Shams-SX well			Shams-NE Well		
	From	To		Top (m)	Bottom (m)	Thick (m)	Top (m)	Bottom (m)	Thick (m)
Sediments surface	–	–	–	0	12.19	12.19	0	9.14	9.14
MARMARICA	15.60	8.40	LIMESTONE	12.19	185.93	173.74	9.14	193.60	184.46
MOGHRA	28.60	15.60	SANDS&SHALE	185.93	519.69	333.76	193.60	524.30	330.70
DABAA	49.60	28.60	SHALE	519.69	754.10	234.41	524.30	760.50	236.20
APOLLONINA	57.60	49.60	LIMESTONE	754.10	830.88	76.78	760.50	839.50	79.00
KHOMAN	68.05	57.60	LIMESTONE	830.88	1184.15	353.27	839.50	1150.30	310.80
ABU ROASH	89.35	68.05	LIME& SHALE& SANDS	1184.15	1904.40	720.25	1150.30	1861.11	710.81
BAHARYIA	97.65	89.35	SANDS&SHALE& LIME	1904.40	2185.11	280.71	1861.11	2127.50	266.39
KHARITA	110.31	97.65	SANDS&SHALE	2185.11	2613.36	428.25	2127.50	2561.50	434.00
ALAMEIN	113.26	110.31	DOLOMITE	2613.36	2713.33	99.97	2561.50	2647.19	85.69
ALAM EL-BUEIB	135.60	113.26	SANDS&SHALE&DOLO	2713.33	3468.93	755.60	2647.19	3484.50	837.31
MASAJID	141.13	135.60	LIMESTONE	3468.93	3524.71	55.78	3484.50	3587.50	103.00
KHATATABA	176.65	141.13	SANDS&SHALE	3524.71	3883.15	358.44	3587.50	3871.00	283.50
RAS QATTARA	199.60	176.65	SANDS&SHALE	3883.15	4114.80	231.65	3871.00	4108.70	237.70

less than 4.0 mg HC/g rock are generally considered to indicate poor generative potential. Following Rock-Eval and TOC analysis, 27 samples were selected for further microscopic examination. Vitrinite reflectance (%VRr) was measured and conducted on the selected samples using a microscope with white light source, photometer and oil immersion objectives.

3.2. Modeling procedure

Basin modelling is widely used to study the burial and thermal histories (Lopatin, 1971; Welte and Yukler, 1981; Waples, 1988, 1994; Burrus et al., 1991; Hermanrud, 1993; Littke et al., 1994; Yalcin et al., 1997; Hakimi et al., 2010). The aim of the numerical

Table 2
Bulk geochemical results of Rock-Eval/TOC analysis with calculated parameters of samples from the Khatatba Formations.

Depth (ft)	TOC Wet%	Rock-Eval Pyrolysis								
		S1 (mg/g)	S2 (mg/g)	S3 (mg/g)	S2/S3 (mg/g)	S1 + S2 (mg/g)	T_{max} (°C)	HI	OI	PI
Shams-2X well										
11,840	1.71	0.19	1.92	1.29	1.50	2.11	446	112	75	0.09
11,960	2.69	0.47	3.85	1.36	2.80	4.32	441	143	51	0.11
12,010	1.65	0.24	1.74	1.37	1.30	1.98	449	105	83	0.12
12,020	1.69	0.18	1.75	1.31	1.30	1.93	447	104	78	0.09
12,120	1.18	0.21	1.19	2.08	0.57	1.4	448	101	176	0.15
12,140	1.49	0.21	1.65	1.65	1.00	1.86	449	111	111	0.11
12,180	2.39	0.2	2.75	1.22	2.30	2.95	448	115	51	0.09
12,210	2.06	0.23	2.42	1.45	1.70	2.65	448	117	70	0.09
12,250	2.9	0.22	4.4	1.27	3.50	4.62	449	152	44	0.09
12,260	2.39	0.2	3.08	1.89	1.60	3.28	448	129	79	0.10
12,270	3.24	0.3	3.47	1.89	1.80	3.77	452	107	58	0.12
12,390	2.97	0.25	3.01	0.31	9.70	3.26	452	101	10	0.09
12,640	6.64	0.57	7.71	0.47	16.4	8.28	455	116	7.0	0.07
12,650	16.47	1.54	28.35	0.67	42.3	29.89	455	172	4.0	0.10
12,730	5.24	0.63	5.58	1.76	3.20	6.21	456	106	34	0.10
Shams-NE Well										
12,310	1.95	0.24	2.17	1.22	1.78	2.41	445	111	63	0.10
12320	1.95	0.24	2.14	1.04	2.10	2.38	443	110	53	0.10
12,340	2.00	0.25	2.29	1.44	1.59	2.54	445	115	72	0.10
12,350	2.42	0.33	3.17	1.26	2.51	3.5	441	131	52	0.09
12,360	1.85	0.27	2.16	1.26	1.71	2.43	443	117	68	0.11
12,370	1.24	0.23	1.31	1.27	1.03	1.54	443	106	102	0.15
12,470	3.77	0.63	6.21	0.6	10.4	6.84	442	165	16	0.09
12,480	4.14	0.5	5.8	0.28	20.7	6.3	454	140	7.0	0.08
12,490	8.67	1.58	19.25	0.69	27.9	20.83	449	222	8.0	0.08
12,500	8.08	1.7	19.04	0.61	31.2	20.74	444	236	8.0	0.08
12,530	9.20	2.07	22.19	0.95	23.4	24.26	449	241	10	0.09
12,540	3.65	0.53	6.94	0.42	16.5	7.47	449	190	12	0.07
12,550	8.76	1.72	22.86	0.69	33.2	24.58	451	261	8.0	0.07
12,570	27.0	4.53	63.8	0.79	80.8	68.33	457	236	3.0	0.07
12,580	24.3	3.79	54.21	0.61	88.9	58	458	223	3.0	0.07
12,590	8.19	1.32	16.21	0.49	33.1	17.53	456	198	6.0	0.08
12,600	18.4	3.85	42.16	0.61	69.1	46.01	453	230	3.0	0.08
12,610	32.5	8.07	71.47	0.88	81.2	79.54	456	220	3.0	0.10
12,620	30.1	5.57	67.58	1.01	66.9	73.15	453	225	3.0	0.08
12,650	29.2	4.2	59.11	2.52	23.5	63.31	453	203	9.0	0.07
12,660	24.2	4.3	54.4	2.32	23.5	58.7	455	225	10	0.07
12,670	22.9	3.66	50.46	1.53	32.9	54.12	457	221	7.0	0.07
12,680	46.9	9.13	89.76	1.65	54.4	98.89	452	191	4.0	0.09
12,690	34.7	6.32	70.56	2.35	30.0	76.88	451	203	7.0	0.08

Table 3
Bulk geochemical results of Rock-Eval/TOC analysis with calculated parameters of samples from the Ras Qattara Formation.

Depth (ft)	TOC Wet%	Rock-Eval Pyrolysis								
		S1 (mg/g)	S2 (mg/g)	S3 (mg/g)	S2/S3 (mg/g)	S1 + S2 (mg/g)	T_{max} (°C)	HI	OI	PI
Shams-2X well										
12,740	4.01	0.44	4.34	1.41	3.08	4.78	454	108	35	0.09
12,790	8.04	1.10	11.6	0.64	18.1	12.7	455	144	8.0	0.09
12,810	16.8	2.41	24.8	0.93	26.7	27.2	456	148	6.0	0.09
12,840	4.32	0.51	4.50	1.02	4.41	5.01	458	104	24	0.10
12,850	3.20	0.25	3.27	0.48	6.81	3.52	456	102	15	0.09
12,860	3.82	0.51	4.19	0.77	5.44	4.70	456	110	20	0.11
12,870	4.93	0.52	4.44	0.87	5.10	4.96	457	90	18	0.10
12,880	5.83	0.71	6.69	0.59	11.3	7.40	456	115	10.	0.10
12,890	8.00	0.88	8.27	0.73	11.3	9.15	456	103	9.0	0.10
12,900	8.96	0.96	8.96	0.86	10.4	9.92	455	100	10	0.10
12,910	12.3	1.65	17.0	0.77	22.1	18.7	458	139	6.0	0.09
12,940	3.04	0.33	3.11	0.62	5.02	3.44	453	102	20	0.10
12,990	4.44	0.56	5.10	0.61	8.36	5.66	454	115	14	0.10
13,350	4.13	0.46	4.06	1.12	3.63	4.52	454	98	27	0.10
Shams NE Well										
12,700	21.21	4.01	45.31	2.55	17.8	49.32	450	214	12	0.08
12,710	29.11	5.59	59.91	2.54	23.6	65.5	452	206	9.0	0.09
12,720	28.81	6.03	60.6	1.89	32.1	66.63	451	210	7.0	0.09
12,730	24.11	4.79	51.07	2.06	24.8	55.86	449	212	9.0	0.09
12,740	29.03	5.58	61.95	2.06	30.1	67.53	450	213	7.0	0.08
12,750	34.67	6.35	73.64	2.31	31.9	79.99	453	212	7.0	0.08
12,760	40.15	7.67	78.54	2.23	35.2	86.21	452	196	6.0	0.09
12,770	53.71	12.61	103.94	1.36	76.4	116.55	449	194	3.0	0.11
12,780	23.01	4.73	54.16	0.78	69.4	58.89	452	235	3.0	0.08
12,790	39.67	8.17	79.52	1.28	62.1	87.69	441	200	3.0	0.09
12,800	24.92	4.25	50.63	0.81	62.5	54.88	445	203	3.0	0.08
12,810	52.32	11.46	96.96	1.29	75.2	108.42	438	185	2.0	0.11
12,860	7.62	1.12	12.56	0.73	17.2	13.68	440	165	10	0.08
12,920	6.79	0.6	6.21	0.64	9.70	6.81	445	91	9.0	0.09
12,950	2.49	0.28	2.92	0.67	4.36	3.2	446	117	27	0.09
12,990	2.23	0.31	2.48	1.09	2.28	2.79	448	111	49	0.11

TOC: Total organic Carbon, wt. %, S1: Volatile hydrocarbon (HC) content, mg HC/g rock, S2: Remaining HC generative potential, mg HC/g rock, S3: carbon dioxide content, mg CO2/g rock, HI: Hydrogen Index = S2 × 100/TOC, mg HC/g TOC, OI: Oxygen Index = S3 × 100/TOC, mg CO2/g TOC, PI: Production Index = S1/(S1 + S2).

modelling was to determine the depth and timing of hydrocarbon generation and expulsion in the two selected wells (Shams-NE and Shams-2X Wells). Burial history, thermal maturity and hydrocarbon generation were reconstructed using PetroMod 1D software following Littke et al. (1993); Poelchau et al. (1997); Yalcin et al. (1997) and Buker et al. (1999). To assess the amount of generated and expelled hydrocarbons from the Jurassic source rocks, the

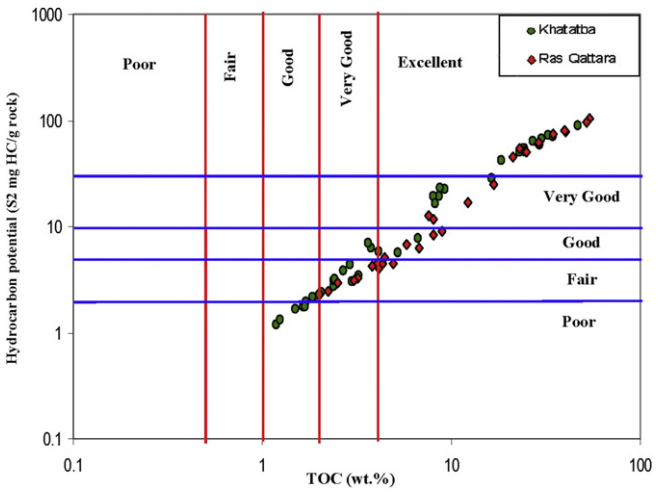

Figure 4. Plot of S2 versus total organic matter (TOC) for the Ras Qattara and Khatatba samples analysed, showing generative source rock potential.

Table 4
Summary of vitrinite reflectance data for studied samples from Jurassic source rocks, Shushan Basin.

Formation	Wells	Depth (m)	Vitrinite reflectance		
			(VRr %)	SD	N
Khatatba Formation	Shams –NE Well	3800.9	0.85	0.08	18
		3816.1	0.85	0.09	19
		3831.3	0.90	0.13	19
		3840.5	0.98	0.07	20
		3849.6	1.04	0.09	30
		3852.7	1.02	0.10	22
		3864.9	1.06	0.10	32
	Shams–2X Well	3605.8	1.02	0.06	18
		3645.4	0.79	0.06	27
		3739.9	0.85	0.10	22
		3810.0	0.93	0.12	13
		3855.7	1.08	0.08	10
		3880.1	1.07	0.04	24
Ras Qattara Formation	Shams –NE Well	3877.1	1.00	0.08	20
		3892.3	1.05	0.09	25
		3898.4	1.08	0.03	25
		3904.5	1.05	0.10	18
		4032.5	0.89	0.15	32
		4072.1	0.96	0.08	13
		4093.5	0.92	0.11	19
	Shams-2X Well	3904.5	1.10	0.04	24
		3935.0	1.12	0.10	27
		3950.2	1.07	0.10	34
		3971.5	1.09	0.10	14
		4023.4	1.05	0.11	18
		4069.1	1.11	0.16	20

VRr % = mean random vitrinite reflectance in oil immersion SD = standard deviation N = quantity of measurements.

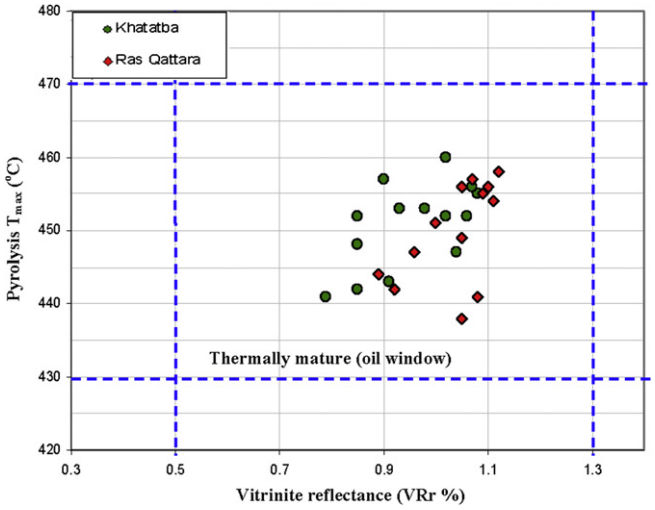

Figure 5. Plot of T_{max} versus vitrinite reflectance values (VRr) values, showing good agreement between T_{max} and vitrinite reflectance (VRr) data.

following input data were defined from exploration wells: event (e.g. deposition, erosion, hiatus or non-deposition), present-day thicknesses, lithology of strata, and present-day depth (Table 1). Geochemical input parameters for modelling include original TOC, type of kerogen and appropriate kinetics. Maturity was calculated using the EASY%Ro model of Sweeney and Burnham (1990).

4. Source rock evaluation

4.1. TOC and Rock Eval pyrolysis data

Total organic carbon (TOC) analysis showed high TOC values of the samples from the Ras Qattara and Khatatba Formations and ranging from 2.23 to 53.71% and from 1.18 to 46.9%, respectively (Tables 2 and 3). Samples from the Ras Qattara and Khatatba Formations have very similar TOC values with slightly higher TOC values in the Ras Qattara samples. In the Rock-Eval pyrolysis analysis, free hydrocarbons (S_1) in the rock and the amount of hydrocarbons (S_2) and CO_2 (S_3) expelled from pyrolysis of kerogen are measured (Tables 2 and 3). In addition, the T_{max} value, which represents the temperature at the point where the S2 peak is the maximum is also determined (Espitalié, 1985). Potential yield ($S_1 + S_2$) values for the samples analysed are high and range between 2 and 98 mg HC/g rock. Samples from Ras Qattara and Khatatba Formations show HI values in the range of 90–261 mgHC/gTOC. T_{max} values of samples from the Ras Qattara and Khatatba Formations are 438–458 °C and 441–458 °C, respectively. Therefore, the remaining potential of these Jurassic shales is good to excellent (Fig. 4), especially for gas generation.

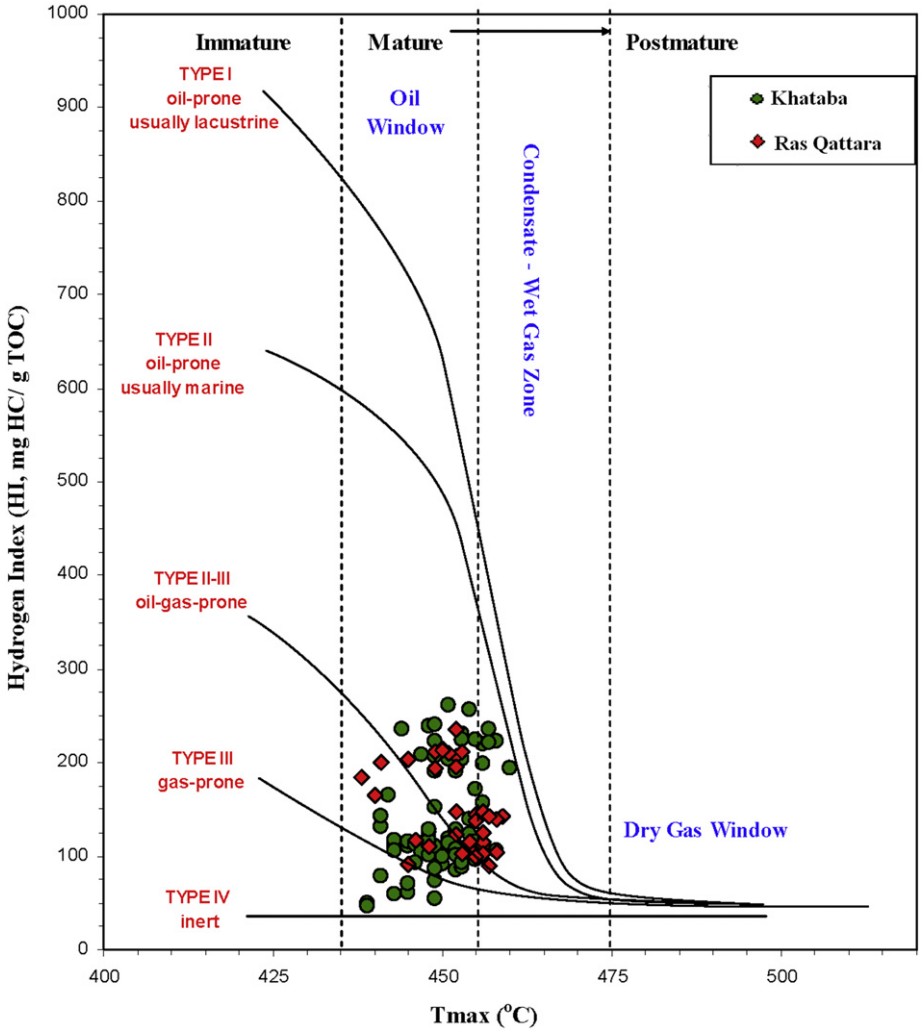

Figure 6. Plot of Hydrogen Index (HI) versus (Rock-Eval) T_{max} values for the samples analysed showing kerogen quality and thermal maturity stages.

4.2. Vitrinite reflectance measurements (VRr)

The mean vitrinite reflectance data for the samples analysed ranges between 0.79 and 1.12% VRr (Table 4), indicating that the samples are thermally mature and have entered the mature to late mature stage of hydrocarbon generation. This is supported by pyrolysis T_{max} values as shown in Fig. 5.

4.3. Type of organic matter

Results of samples collected from Ras Qattara and Khatatba Formations were plotted in the HI versus T_{max} diagram (Mukhopadhyay et al., 1995), which is used to determine the kerogen type and maturity (Fig. 6). T_{max} values may change with respect to depend not only on maturity but also may be influenced by kerogen type (Hunt, 1996). Thus the maturity windows on this diagram are approximately only. Samples from the different formations were plotted in the HI − T_{max} diagram, from which it is seen that most samples generally plot in the mature zone of Type III and Type II-III kerogen (Fig. 6). The type of organic matter has also been classified according to the modified van Krevelen plot of whole rock Hydrogen Index (S2/TOC × 100) and Oxygen Index (S3/TOC × 100) (Tissot and Welte, 1984; Bordenave, 1993) shown in Fig. 7. Most of the studied samples plot in the low Hydrogen Index area (90–110 mgHC/gTOC) and some of the samples plot at relatively highest in the moderate Hydrogen Index area (235–261 mgHC/gTOC). This suggests that the organic matter in the samples collected from the Ras Qattara and Khatatba Formations contains predominantly Type III kerogen (gas prone) and mixed Type II-III kerogen (oil-gas prone), which is in agreement with the previous plot.

4.4. Thermal maturity of organic matter

Organic maturity was determined using vitrinite reflectance data (VRr) and Rock-Eval pyrolysis T_{max} values. Top and bottom of oil and gas (windows) vary with the type of organic matter, ranging from 0.5% to 1.0% VRr and 1.3–3.5% VRr, respectively (Tissot and Welte, 1984; Espitalié, 1985). Generally, vitrinite reflectance values increase with depth due to an increase in temperature and increasing age of the rock with depth. Samples analysed contain Type III and Type II-III kerogen and show vitrinite reflectance values generally between 0.79% 1.12% VRr (Table 4), which is peak to late-mature stage. The distribution of vitrinite reflectance (VRr) data suggests that the Jurassic samples are sufficiently thermally mature (oil window) for hydrocarbon generation (Fig. 5). The thermal maturity of organic matter in the analysed samples is also evaluated based on the T_{max} of the S_2 peak. The pyrolysis T_{max} values for the studied samples (438–458 °C) indicate that the Jurassic Ras Qattara and Khatatba Formations in the basin are early to late mature (Fig. 6).

4.5. Potential for hydrocarbon generation

In this study, Rock-Eval/TOC analyses indicate that very good generative potential is found in the Jurassic Ras Qattara and Khatatba sediments. The Ras Qattara and Khatatba Formations samples have high TOC contents (>2.0 wt. %) and pyrolysis S_2 yields are sometimes great than 100 mg HC/g rock. Therefore, these sediments can be regarded as good to excellent potential source rocks for hydrocarbons based on the TOC content and pyrolysis S_2 yields (Fig. 4). Samples of Jurassic Ras Qattara and Khatatba Formations that contain Type III kerogen can generate predominately gas, which is supported by low pyrolysis S_1 yields. The low pyrolysis S_1 yields are commonly observed in coals and type III kerogen bearing rocks (Littke and Leythauser, 1993).

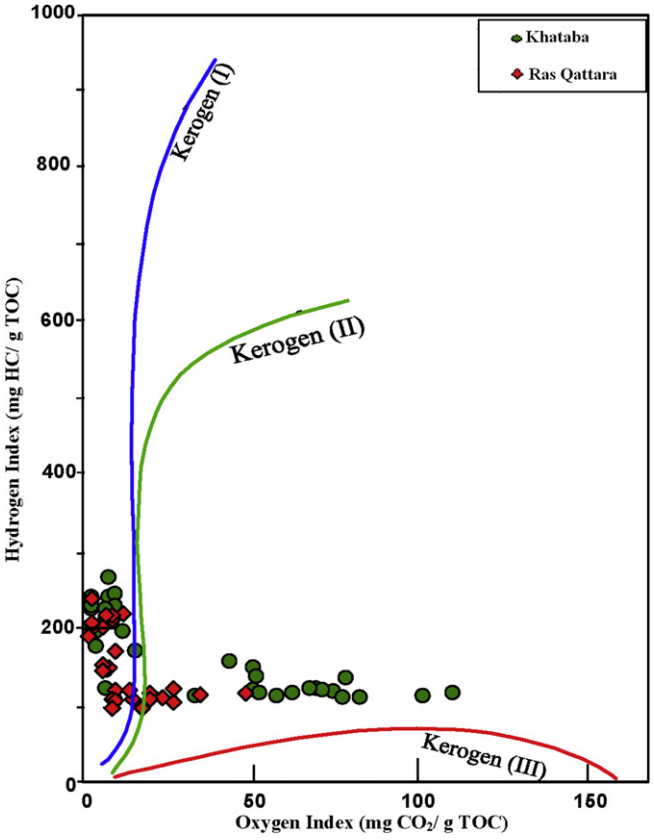

Figure 7. Plot of oxygen index versus hydrogen index for the Ras Qattara and Khatatba samples.

On the other hands, the analysed samples with hydrogen indices greater than 200 mg HC/g TOC that contain (mixed Type II-III organic matter kerogen) can generate oil and gas if they are subjected to sufficient burial and heating. In this respect, both the Ras Qattara and Khatatba samples have a good hydrocarbon generation. In addition, the plot of production index (PI) versus T_{max} (Fig. 8) can be used to show the origin of hydrocarbons produced. Based on this

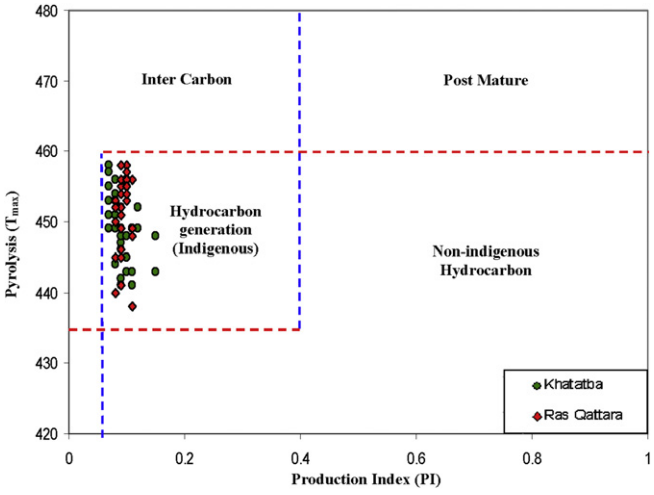

Figure 8. Plot of T_{max} versus production index (PI), showing the maturation and nature of the hydrocarbon products of the Ras Qattara and Khatatba samples analysed.

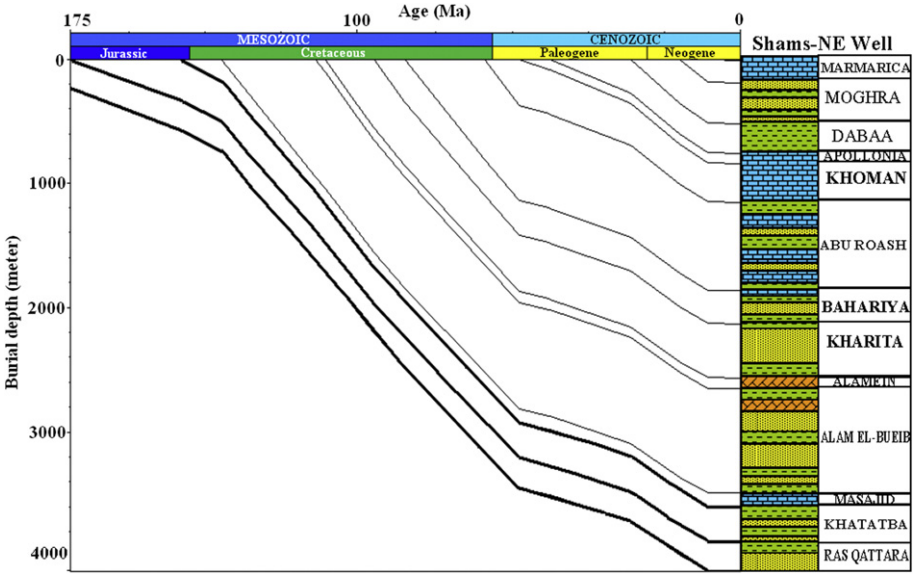

Figure 9. Burial history curves for Shams NE- well, Shams field in the Shushan Basin (Bold lines for Ras Qattara and Khatatba Formations).

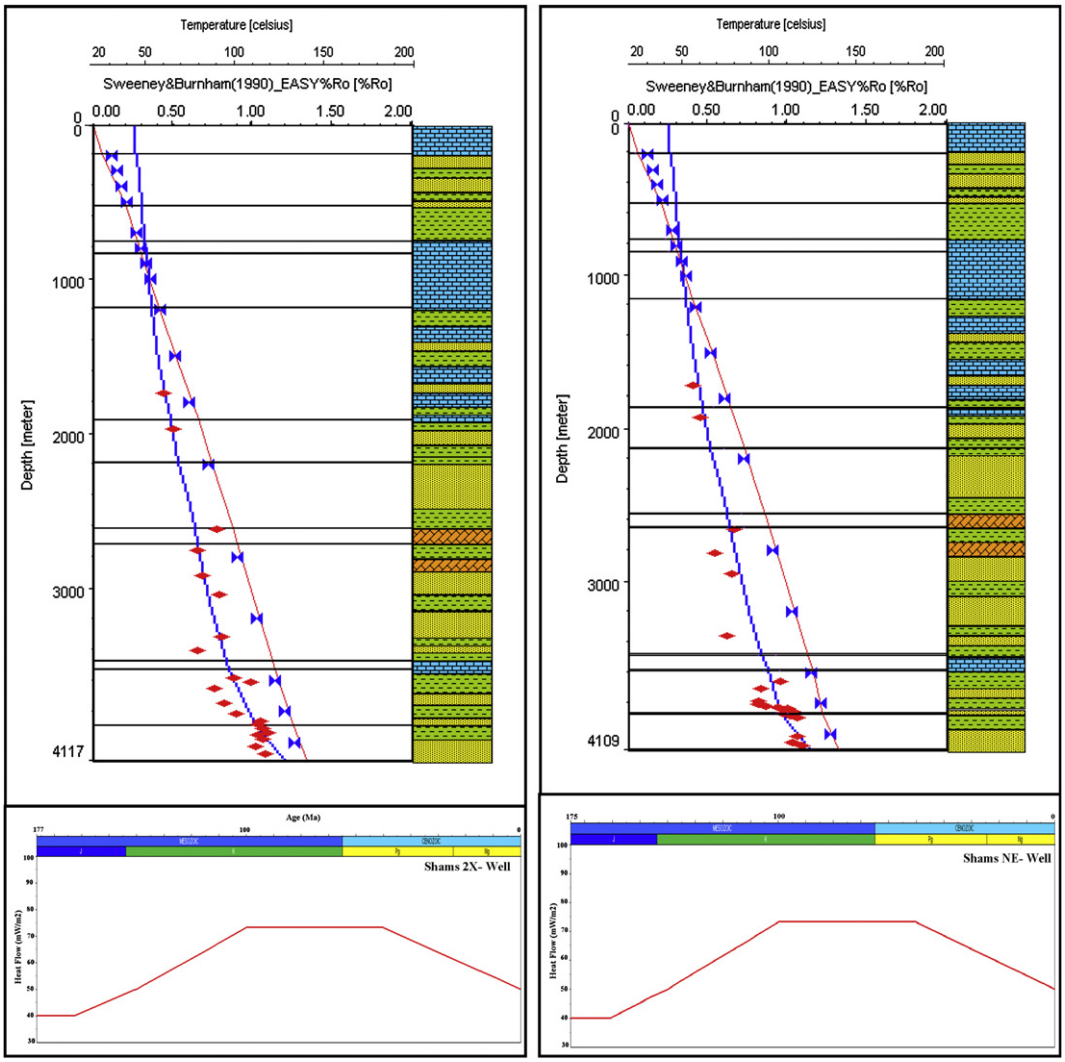

Figure 10. Plots of calculated (lines) and measured (symbols) vitrinite reflectance values and corrected borehole temperatures versus depth for studied wells; the lower diagrams for each well show the assumed heat-flow history as used for the calculation.

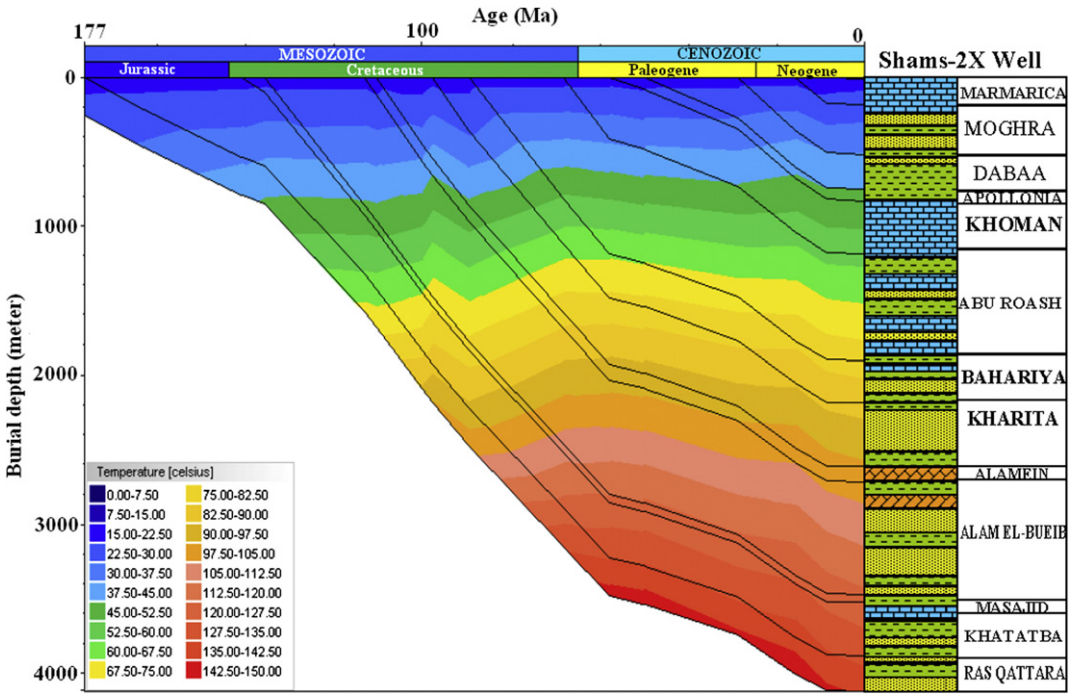

Figure 11. Burial history curves with palaeo-temperature zones in studied well Shams 2X, Shams Field, Shushan Basin.

plot, the Ras Qattara and Khatatba samples are thermally mature and the hydrocarbons are expected to be indigenous rather than migrated hydrocarbons (Fig. 8).

5. Numerical modeling

5.1. Burial history

The tectonic evolution of the region has significantly influenced burial and thermal history of the study area. An understanding of local subsidence and thermal history is necessary in order to predict timing of hydrocarbon generation. In the study area, subsidence rate can be estimated using the deposition age and the present thickness for the formations which are penetrated by the studied wells. The burial history at the studied wells is very similar, which example is shown in Fig. 9. The subsidence during the Jurassic (198–144 Ma) was characterized by relatively low burial rates of about9.8 m (32 ft) per million years leading to a present thickness of about 645.9 m (2119 ft). Following this phase, the subsidence rate increased to about 32.9 m (108 ft) per million years with present thickness of about 1283.8 m (4212 ft) for the Lower Cretaceous (144–104 Ma). The Late Cretaceous (104–66 Ma) was characterized by higher burial rates of about 34.7 m (114 ft) per million years leading to a present thicknesses of about 1354.2 m (4443 ft). The end of Cretaceous to Cenozoic was characterized by relatively low average subsidence rates of about 12.5 m (41 ft) per million years. A total thickness of 830.3 m (2724 ft) of sediment was deposited.

5.2. Thermal history and palaeo-temperature data

Analysis of the tectonic evolution of the Shoushan Basin and the recent heat flow distribution were used for a qualitative reconstruction of the basin's thermal history. A basin's thermal history is controlled by heat flow from the mantle, radiogenic heat produced in the crust and regional-scale hydrodynamic flows (Allen and Allen, 1990; Lachenbruch, 1970). Increased heat flow during rifting is due to lithospheric thinning. The heat flow in an active rift averages about 80 mW/m^2 (Allen and Allen, 1990), decreasing to an average value of about 50 mW/m^2 during post-rift thermal subsidence. In this study, analysis of the influence of the tectonic evolution in the basin on the heat flow distribution through time was made using 1D modeling. The thermal history during the tectonic development was calibrated with vitrinite reflectance data from the Cretaceous and Jurassic sediments. The calibration curves for the studied wells are presented in Fig. 10, which shows plots of vitrinite reflectance data and corrected bottom-hole temperature versus depths. A good match between measured (symbols) and calculated (lines) vitrinite reflectance values was generally achieved. The heat flow histories used in the calculations are also plotted in Fig. 10. Although heat flow is vital input parameter in basin modeling, it is commonly difficult to define this value for the geological past. Therefore, the reconstruction of the thermal history of the basin is always simplified and is usually calibrated against profiles of maturity (e.g. vitrinite reflectance). In this 1 D model, the heat flow values were estimated and calibrated using measured vitrinite reflectance (%VRr) data. In the studied wells, heat flow values range between 40 and 73 mW/m^2, which are used for numerical modeling in the study area (Fig. 10). The studied wells reach maximum burial and maximum temperature at present day, therefore, the heat flow can only be determined for the last few million years. Jurassic heat flows were kept at 40 mW/m^2 and increased to 73 mW/m^2 during the late Cretaceous-Early Tertiary then decreased to 50 mW/m^2 at the present day. The applied heat flows lead to a good match between optical measured and calculated vitrinite reflectance values (Fig. 10). The corrected bottom-hole temperatures can be matched with the present day heat flow values. Different heat flows at the studied wells were required to achieve a good fit between corrected measured bottom-hole temperatures and calculated temperatures. However, these variations are not required to match the measured vitrinite reflectance values. Calibration of the Mesozoic thermal history, despite scarcity

of data, allows an interpretation of the regional maturity trend to be made. The vitrinite reflectance of the kerogen in the Jurassic sediments indicates thermal maturities corresponding to mature-late mature stages of hydrocarbon generation (Table 4).

Thermal models also incorporate palaeo-temperature histories which can be reconstructed from borehole temperatures (heat flow history and heat conductivity). Temperatures recorded in the studied wells are generally not in equilibrium and were corrected for the circulation of drilling fluids. The values increase systematically with depth from a surface temperature. The studied wells reached maximum temperatures at the present day (Fig. 11).

5.3. Timing of hydrocarbon generation of the Jurassic source rocks

The timing of hydrocarbon generation from the Jurassic Ras Qattara and Khatatba Formations in the studied wells was analysed and determined based on temperature and maturation history. Petroleum generation stages were calculated assuming mainly Type III and mixed Type II-III kerogen and using a reaction kinetic data set based on Burnham (1989). The modelled hydrocarbon generation of the studied wells is shown in Fig. 12. This model shows that the corresponding to onset of the oil window (0.50–0.60% VRr) of the Jurassic source rocks was during Late Cretaceous at depths greater than 2000 m (6561.7 ft) (Fig. 12). The

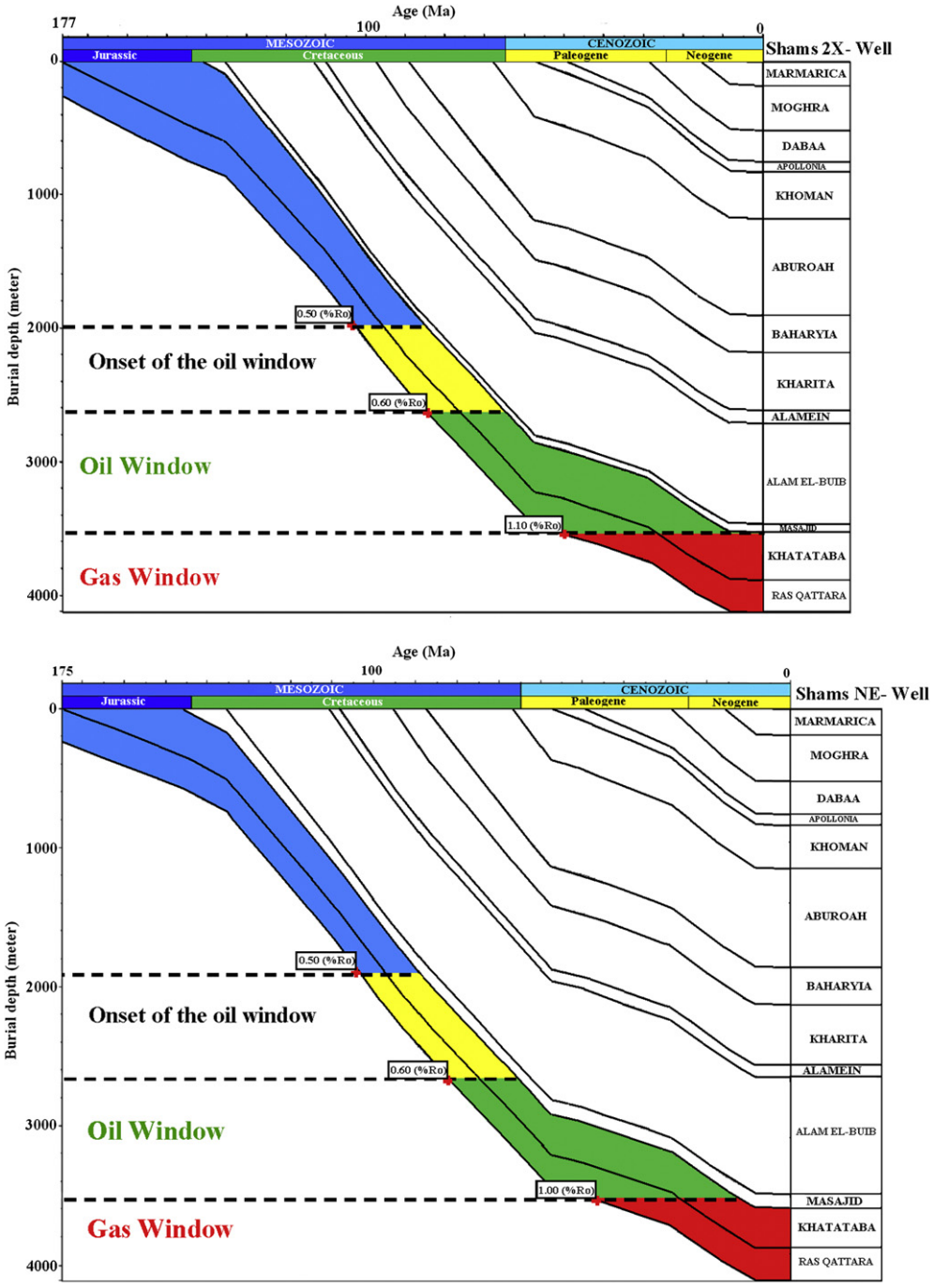

Figure 12. Burial history curves with hydrocarbon zones for the Ras Qattara and Khatatba Formations in the studied wells, Shams Field, Shushan Basin.

Jurassic source rocks reached late mature stages at end of Late Cretaceous and the gas window in the Tertiary (Fig. 12); accordingly the hydrocarbon generation (oil and gas) started in the Late Cretaceous and peak hydrocarbon generation occurred during the Tertiary (Figs. 12, 13a and b). The amount of hydrocarbon generation (oil and gas) was evaluated based on the transformation ratio and kerogen type. The transformation ratio is defined as the ratio of the amount of generated hydrocarbons to the total amount of hydrocarbons that the kerogen is capable to generate.

The oil generation curves (Fig. 13) for the studied wells show that significant oil generation from the Jurassic sediments started at the Late Cretaceous (85–100 Ma age). For the Jurassic Khatatba, the

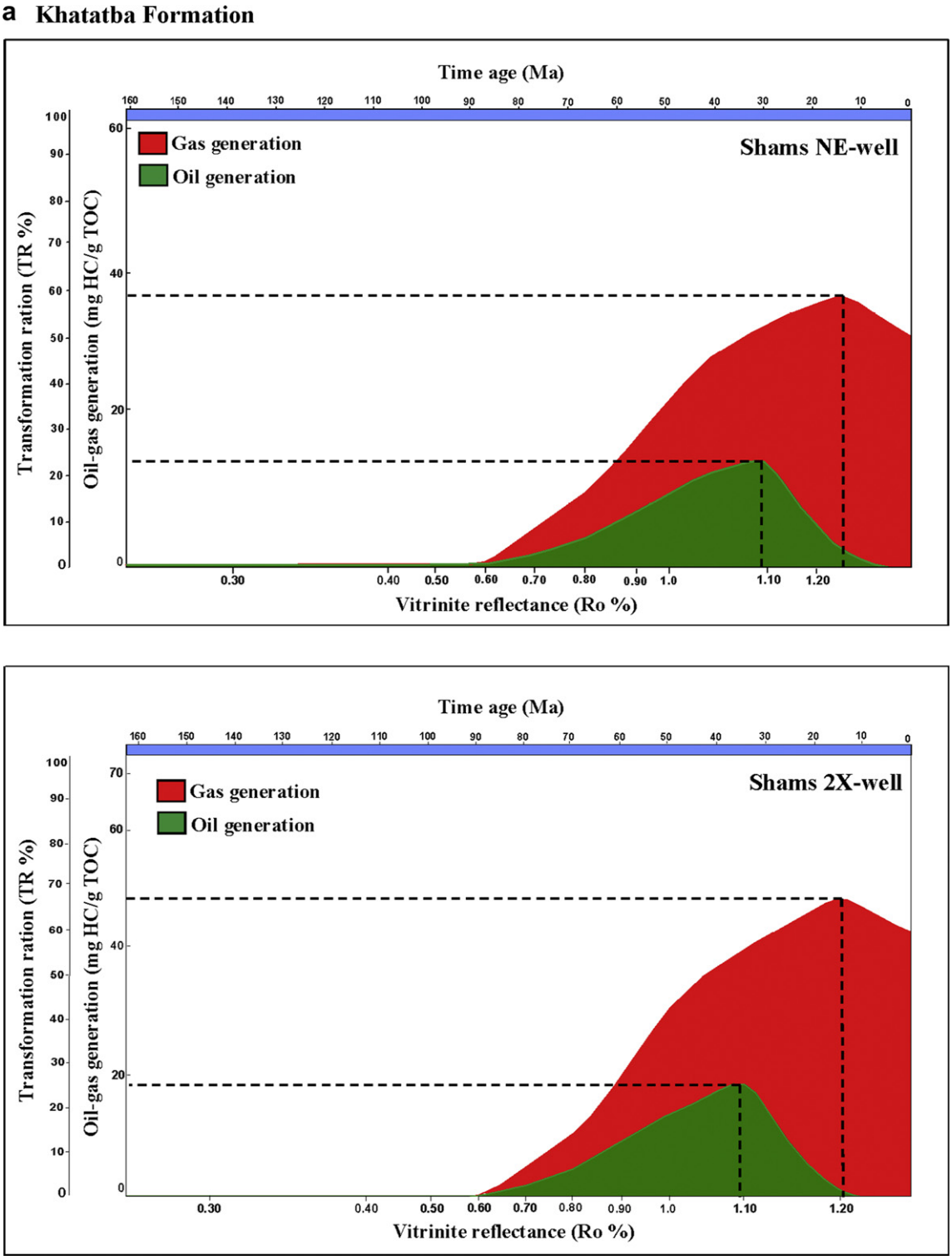

Figure 13. Calculated (cumulative model) of transformation ratios and hydrocarbon generation from organic matter in the Ras Qattara (a) and Khatatba (b) Formations in the studied wells, Shushan Basin.

b Ras Qattara Formation

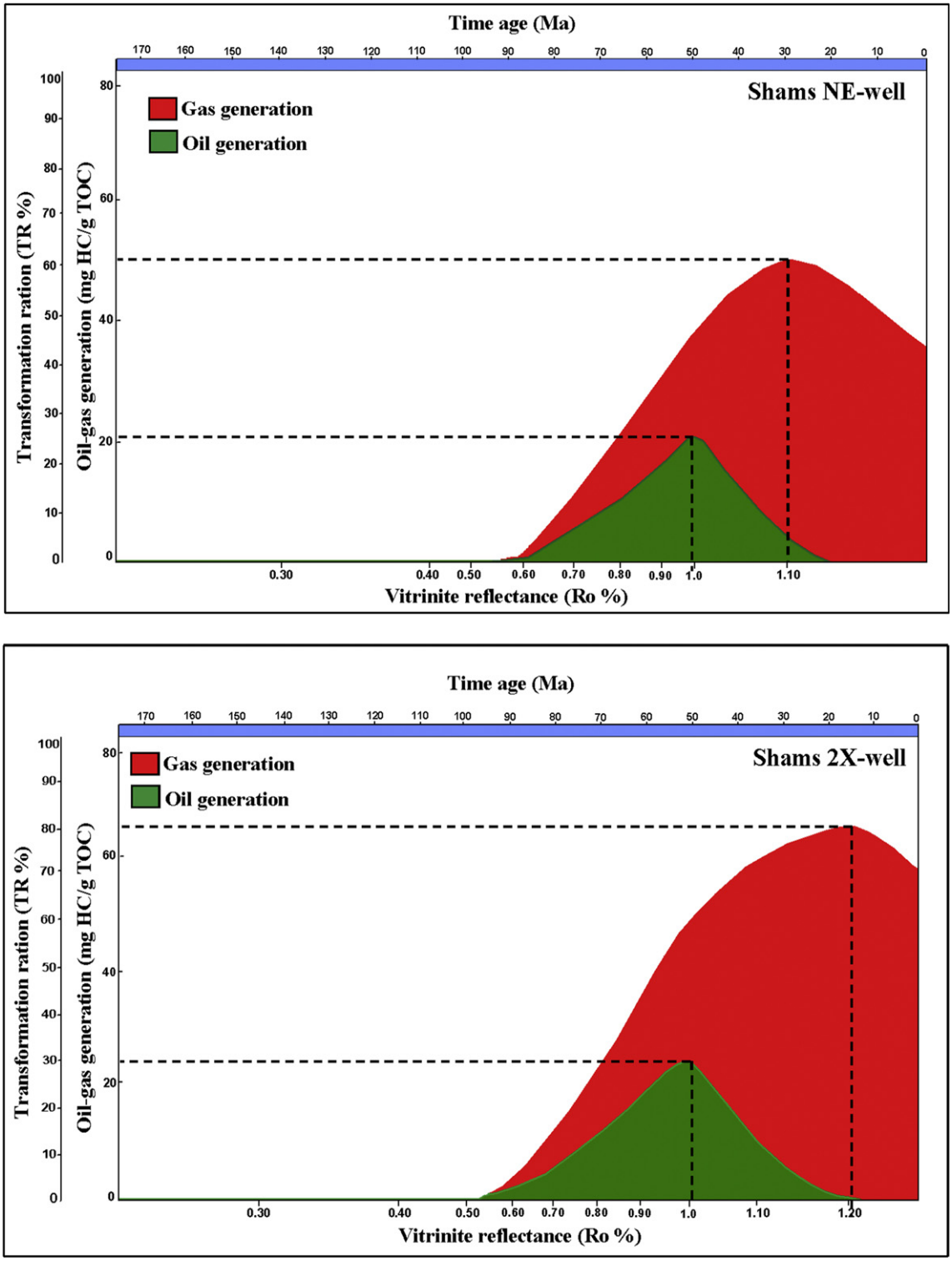

Figure 13. (*continued*).

transformation ratio reaches 17–21% during the Paleogene (35–30 Ma age), with oil as the main product. Gas generation in this region can be expected from reaching the maximum transformation ratio (38%–48%) and occurred during the Neogene (12 Ma age; Fig. 13a). Meanwhile, the higher transformation ratio of Jurassic Ras Qattara organic matter has been calculated (Fig. 13b). The transformation ratio for the main oil generation reaches 20%–25% during the Paleogene (50 Ma age). In contrast the transformation ratio required for reaching maximum gas generation occurred during Paleogene to Neogene (30–12 Ma age; Fig. 13b).

For the above maturity model, the hydrocarbon generation potential from the Ras Qattara and Khatatba sediments is mainly gas with some oil generation (Fig. 13).

In the study area, the thickness of the Ras Qattara and Khatatba Formations in borehole sections varies from 280 to 360 m (930–1176 ft) and 231–235 m (760–780 ft), respectively. The Ras Qattara and Khatatba sediments have a good to excellent hydrocarbon potential with mainly gas generation potential. Therefore, the Ras Qattara and Khatatba Formations are effective hydrocarbon source rocks in the Shams field. This is in agreement with the production of the field, which is mainly gas production (Fig. 1).

6. Conclusions

The Jurassic Ras Qattara and Khatatba Formations are important oil and gas source rocks in the Shushan Basin, Western Desert, Egypt. Samples have been collected from both formations to study the organic geochemical and some organic petrographic characteristics. The sediments of Ras Qattara and Khatatba Formations contain types III and mixed type II-III kerogen with Hydrogen Index (HI) values ranging between 100 and 260 mg HC/g TOC. Vitrinite reflectance data shows that the Ras Qattara and Khatatba sediments have reached the mature to late mature stages for hydrocarbon generation, consistent with Rock-Eval pyrolysis T_{max} values. Based on these data, the Jurassic sequences have attained sufficient burial depth and thermal maturity for significant hydrocarbon generation. Numerical modeling of various wells indicates that the Jurassic source rocks entered the mature to late mature stages for hydrocarbon generation during Late Cretaceous to Tertiary. The depth of oil window ranges from 2630 to 2650 m (8628.6–8694.2 ft), while the depth of late oil/early gas generation transition zone was penetrated in the depths of range 3530–3560 m (11581.4–11679.8 ft) in the studied wells. For the assumed maturity model, the hydrocarbon generation potential is mainly gas and oil. The hydrocarbon generation phase started during the Late Cretaceous and peak oil with significant gas was generated during early Tertiary (Paleogene), reaching maximum rates of gas generation during Neogene.

Acknowledgements

The authors would like to thank Khalda Oil Company, Egypt for providing the data and samples for this study. The authors are grateful to the Department of Geology, University of Malaya for providing facilities to complete this research. CCOP is acknowledged for providing the IES PetroMod Basin Modeling software. Special thanks are offered to Peter Abolins for his helpful comments on an earlier version of the manuscript. The authors would also like to thank anonymous reviewers who provided useful comments that improved the revised manuscript.

References

Allen, P.A., Allen, J.R., 1990. Basin Analysis Principles and Applications. Blackwell Scientific Publications, Oxford.

Alsharhan, A.S., Abd El-Gawad, E.A., 2008. Geochemical characterization of potential Jurassic/Cretaceous source rocks in the Shushan Basin, north Western Desert, Egypt. Journal of Petroleum Geology 31, 191–212.

Barakat, M.G., Darwish, M., Abdelhamid, M.L., 1987. Hydrocarbon source rock evaluation of the upper Cretaceous (Abu Roash formation) east Abu Gharadig area, North Western Desert, Egypt. Earth Science Journal 1, 120–150. Ain Shams University.

Bordenave, M.L., 1993. Applied Petroleum Geochemistry. Editions Technip, Paris.

Buker, C., Littke, R., Welte, D.H., 1999. 2D-modelling of thermal evolution of Carboniferous and Devonian sedimentary rocks of the eastern Ruhr Basin and northern Rheinish Massif, Germany. Zeitschrift der deutschen Geologischen Gesellschaft 146, 321–339.

Burnham, A. K., 1989. A simple kinetic model of petroleum formation and cracking. Lawrence Livermore National Laboratory Report UCID-21665.

Burrus, J., Kuhfuss, A., Doligez, B., Ungerer, P., 1991. Are numerical models useful in reconstructing the migration of hydrocarbons? In: England, W.A., Fleet, A.J. (Eds.), A Discussion Based on the Northern Viking Graben Petroleum Migration, vol 59 Geological Society, London, pp. 89–109. Special Publication.

Dolson, J.C., Shann, M.V., Matbouly, S.I., Hammouda, H., Rashed, R.M., 2001. Egypt in the twenty first century: petroleum potential in offshore trends. GeoArabia 6, 211–230.

El Ayouty, M.K., 1990. Petroleum geology. In: Said, R. (Ed.), The Geology of Egypt, pp. 567–599. A.A. Balkema, Rotterdam.

El Shazly, E.M., 1977. The geology of the Egyptian region. In: Kanes, A.E.M., Stehli, F.G. (Eds.), The Ocean Basins and Margins. Plenum, New York, pp. 379–444.

El-Nadi, M., Harb, F., Basta, J., 2003. Crude oil geochemistry and its relation to the potential source beds of some Meleiha oil fields in the north Western Desert, Egypt. Petroleum Science and Technology Journal 21, 1–28.

Espitalié, J., 1985. Use of Tmax as a maturation index for different types of organic matter-comparison with vitrinite reflectance. In: Burrus, J. (Ed.), Thermal Modeling in Sedimentary Basins. Editions Technip, Paris, pp. 475–496.

Espitalié, J., Laporte, J.L., Madec, M., Marquis, F., Leplat, P., Pauletand, J., Boutefeu, A., 1977. Methode rapide de caracterisation des roches meres, de leur potential petrolier et de leur degre d'evolution. Revue de l'Institut Francais du Petrole 32, 23–42.

Ghanem, M., Sharaf, L., Hussein, S., El-Nadi, M., 1999. Crude oil characteristics and source correlation of Jurassic and Cretaceous oil in some fields, north Western Desert, Egypt. Bulletin of Egyptian Society of Sedimentology 7, 85–98.

Hakimi, H.H., Abdullah, W.H., Shalaby, M.R., 2010. Organic Geochemistry, burial history and hydrocarbon generation modelling of the Upper Jurassic Madbi Formation, Masila Basin, Yemen. Journal of Petroleum Geology 33, 299–318.

Hantar, G., 1990. North Western Desert. In: Said, R. (Ed.), The Geology of Egypt. Balkema, Rotterdam, pp. 293–319.

Hermanrud, C., 1993. Basin modelling techniques-an overview. In: Dore, A.G., Augustson, J.H., Hermanrud, C., Stewart, D.J., Sylta, O. (Eds.), Basin Modelling: Advances and applications. Norwegian Petroleum Society (NPF), pp. 1–34. Special Publication.

Hunt, J.M., 1996. Petroleum Geochemistry and Geology, second ed.. Freeman, San Francisco.

Kerdany, M.T., Cherif, O.H., 1990. Mesozoic. In: Said, R. (Ed.), The Geology of Egypt. Balkema, Rotterdam, pp. 407–438.

Khaled, K.A., 1999. Cretaceous source rocks at Abu Gharadig oil and gas field, north Western Desert, Egypt. Journal of Petroleum Geology 22, 377–395.

Lachenbruch, A., 1970. Crustal temperature and heat productivity: implications of the linear heat flow relation. Journal of Geophysical Research 75, 3291–3300.

Littke, R., Leythauser, D., 1993. Migration of oil and gas in coals. American Association Petroleum Geologist Studies in Geology 38, 219–236.

Littke, R., Sachsenhofer, R.F., Hantschel, T., Wygrala, B., 1993. Absenkungsgeschichte und Kohlenwasserstoffbildung im Oberkarbon des westlichen Emslandes-Eine Simulationsstudie. DGMK Forschumgsberichte project 459–2, Hamburg, p. 114.

Littke, R., Buker, C., Luckge, A., Sachsenhofer, R.F., Welte, D.H., 1994. A new evaluation of palaeo-heat flows and eroded thicknesses for the Carboniferous Ruhr Basin, western Germany. International Journal Coal Geology 26, 155–183.

Lopatin, N.V., 1971. Temperature and geologic time as factors in coalification. Izvestiya Akademii Nauk SSSR, Seriya Geologicheskaya 3, 95–106.

Mesherf, W.M., Abdel Bki, S.H., AbdelHady, H.M., Soliman, S.A., 1980. Magnetic trend analysis in the Northern part of Arabian-Nubian Shied and its tectonic implications. Annual Geological Survey, Egypt 10, 939–953.

Mukhopadhyay, P.K., Wade, J.A., Kruge, M.A., 1995. Organic facies and maturation of Jurassic/Cretaceous rocks, and possible oil-source rock correlation based on pyrolysis of asphaltenes, Scotion Basin, Canada. Organic Geochemistry 22, 85–104.

Peters, K.E., 1986. Guidelines for evaluating petroleum source rock using programmed pyrolysis. American Association of Petroleum Geologists Bulletin 70, 318–386.

Peters, K.E., Cassa, M.R., 1994. Applied source rock geochemistry. In: Magoon, L.B., Dow, W.G. (Eds.), The Petroleum System – From Source to Trap, vol 60. American Association of Petroleum Geologists, Memoir, pp. 93–120.

Poelchau, H.S., Baker, D.R., Hantscgel, T., Horsfield, B., Wygrala, B., 1997. Basin Simulation and the Design of the Conceptual Basin Model. In: Welte, D.H., Horsfield, B., Baker, D.R. (Eds.), Petroleum and basin evolution. Springer, Berlin.

Sharaf, L.M., 2003. Source rock evaluation and geochemistry of condensates and natural gases, offshore Nile delta, Egypt. Journal of Petroleum Geology 26, 189–209.

Sweeney, J.J., Burnham, A.K., 1990. Evaluation of a simple model of vitrinite reflectance based on chemical kinetics. American Association of Petroleum Geologists Bulletin 74, 1559–1570.

Tissot, B.P., Welte, D.H., 1984. Petroleum Formation and Occurrence, second ed. Springer Verlag, Berlin, p. 699.

Waples, D.W., 1988. Time and temperature in petroleum formation: application of Lopatin's method to petroleum exploration. American Association of Petroleum Geologists Bulletin 64, 916–926.

Waples, D.W., 1994. Maturity modelling: thermal indicators, hydrocarbon generation, and oil cracking. In: Magoon, L.B., Dow, W.G. (Eds.), The Petroleum System-from Source to Trap, vol 60. American Association of Petroleum Geologists Bulletin, pp. 285–306.

Welte, D.H., Yukler, A., 1981. Petroleum origin and accumulation in basin evolution - a quantitative model. American Association of Petroleum Geologists Bulletin 65, 1387–1396.

Yalcin, M.N., Littke, R., Sachsenhofer, R.F., 1997. Thermal History of Sedimentary Basins. In: Welte, D.H., Horsfield, B., Baker, D. (Eds.), Petroleum and basin evaluation. Springer, Berlin, pp. 73–167.

Zein El-Din, M.Y., Abd El-Gawad, E.A., El-Shayb, H.M., Haddad, I.A., 2001. Geological studies and hydrocarbon potentialities of the Mesozoic rocks in Ras Kanayis onshore area, North Western Desert, Egypt. Annals of the Geological Survey of Egypt, XXIV, 115–134.